

# On the analytical soliton approximations to fractional forced Korteweg–de Vries equation arising in fluids and plasmas using two novel techniques

Weam Alhejaili<sup>1</sup>, Emad A Az-Zo'bi<sup>2</sup>, Rasool Shah<sup>3</sup> and S A El-Tantawy<sup>4,5</sup>

<sup>1</sup>Department of Mathematical Sciences, College of Science, Princess Nourah bint Abdulrahman University, PO Box 84428, Riyadh 11671, Saudi Arabia

<sup>2</sup>Department Mathematics and Statistics, Mutah University, Al-Karak, Jordan

<sup>3</sup>Department of Computer Science and Mathematics, Lebanese American University, Beirut, Lebanon

<sup>4</sup>Department of Physics, Faculty of Science, Port Said University, Port Said 42521, Egypt

<sup>5</sup>Department of Physics, Faculty of Science, Al-Baha University, Al-Baha P.O. Box 1988, Saudi Arabia

E-mail: [tantawy@sci.psu.edu.eg](mailto:tantawy@sci.psu.edu.eg)

Received 10 March 2024, revised 21 April 2024

Accepted for publication 4 June 2024

Published 5 July 2024



CrossMark

## Abstract

The current investigation examines the fractional forced Korteweg–de Vries (FF-KdV) equation, a critically significant evolution equation in various nonlinear branches of science. The equation in question and other associated equations are widely acknowledged for their broad applicability and potential for simulating a wide range of nonlinear phenomena in fluid physics, plasma physics, and various scientific domains. Consequently, the main goal of this study is to use the Yang homotopy perturbation method and the Yang transform decomposition method, along with the Caputo operator for analyzing the FF-KdV equation. The derived approximations are numerically examined and discussed. Our study will show that the two suggested methods are helpful, easy to use, and essential for looking at different nonlinear models that affect complex processes.

Keywords: forced fractional KdV equation, Caputo operator, Yang homotopy perturbation method, Yang transform decomposition method, solitons

## 1. Introduction

Fractional calculus (FC) and fractional order mathematical models have gained substantial popularity in numerous studies for modeling diverse applications in fluid mechanics, physics of plasmas, engineering, and applied sciences. This is primarily attributed to their capacity to effectively and comprehensively represent various issues and applications. The available literature encompasses a wide range of studies, including those focused on modeling biological phenomena and diseases [1, 2], modeling diffusive type circuits [3, 4], conducting an extensive survey on the applications of FC and fractional order derivative-based techniques in computer vision [5], and investigating sensors, analog, and digital

filters [6]. The fundamental framework for FC that several pioneers recommended, as well as their perspectives on generalized calculus. FC has been used in various fields where the fascinating and simulating implications linked with temporal and hereditary features may be found [7–12]. The solution of fractional differential equations that represent complex issues in everyday life is crucial for uncovering their physical core.

Fractional partial differential equations (PDEs) can address intricate engineering and physical issues more effectively than typical integer-order PDEs, showcasing the superior capabilities of fractional PDEs (FPDEs) as demonstrated in references [13–16]. As well as their ability in modeling the complex systems related to the genetic or

memory properties [17–20]. Also, an essential advantage over traditional differential equations is their handling of non-local interactions and long-term time dependence.

One of the PDEs that describes a broad spectrum of physical nonlinear phenomena as well as engineering materials is the well-known Korteweg–de Vries (KdV) equation [21–26]. This equation and its family, whether it contains third-order dispersion [27–29] or fifth-order dispersion [30–32] or other physical effects such as collision and viscosity forces, have effectively elucidated numerous nonlinear structures that emerge and propagate in diverse physical and engineering systems, including fluid physics and plasma physics. It has been widely used, especially in interpreting soliton and cnoidal waves propagating in various plasma systems [33–36]. Furthermore, it succeeded in explaining some ambiguity that may appear in the properties of soliton and shock waves that propagate in numerous plasma models. Many researchers have demonstrated that this ambiguity may be attributed to the fact that these models may encompass various physical effects that influence the dynamics of these waves, including the collisions between plasma charges particles and/or neutral atoms as well as the viscosity of some charged plasma particles, and many other physical effects [37–44].

The forced KdV (FKdV) equation was utilized to examine the influence of bottom configurations on free-surface waves in a two-dimensional channel flow. Studying shallow-water waves highlights the significance of bottom topography in determining wave motion characteristics [45, 46]. Waves with a wavelength in water less than one-quarter of their actual wavelength are categorized as shallow or long waves. As the bottom topography becomes more intricate, the interaction between it and solitary waves (SWs) unveils a rich tapestry of dynamic characteristics within the free surface waves. The free surface waves of a two-dimensional channel flow have been studied in cases where the stiff channel bottom has certain obstructions and for an incompressible and inviscid fluid [47, 48]. When fluid flows over an obstruction, the KdV equation's estimated forcing can be used to show how the free surface develops. When discussing the nonlinear Schrödinger equation and the nature of the sine Gordon equation, the FKdV equation is essential. The model above exhibits numerous applications in tightly interconnected domains of mathematics and physics. This equation is regarded as a vital tool for research into atmosphere dynamics, geostrophic turbulence, and magneto-hydrodynamic waves, to name a few [49, 50]. The study yields promising findings about several physical phenomena, such as the propagation of shallow-water waves over rocks, the occurrence of tsunami waves over obstacles, the interaction between oceanic stratified flows and topographic impediments, and the study of acoustic waves on a crystal lattice.

This article incorporates the FKdV equation, which was first proposed and refined by Wu in 1987 [51], along with the free water surface elevation  $\Phi \equiv \Phi(X, T)$  observed during

critical flow over a hole from the undisturbed water level

$$\frac{1}{c} \partial_T \Phi + \left[ (\mathcal{F}_r - 1) - \frac{3}{2} \frac{\Phi}{h} \right] \partial_X \Phi - \frac{1}{6} h^2 \partial_X^3 \Phi = \frac{1}{2} \partial_X f(X), \quad (1)$$

with

$$f(X) = \frac{\rho_a(X)}{\rho g} + b(X),$$

where  $f(X)$  represents the externally forcing term, “ $h$ ” indicates the sea water depth, and  $\mathcal{F}_r$  represents the Froude number, which is also known as the critical parameter. Here, the surface air pressure is denoted by  $\frac{\rho_a(X)}{\rho g}$ , and stiff bottom topography is specified by  $b(X) = (-0.1e^{-\frac{X^n}{4}} - 1)$ . In equation (1), the Froude number ( $\mathcal{F}_r$ ) is significant hence its value reveals the type of critical flows over the localized restriction. Generally, the flow is classified as subcritical, supercritical, and transcritical for values less than, greater than, and equal to 1, respectively. Two different types of holes, namely those for  $n=2$  and  $n=8$ , were explored in the stiff bottom topography  $b(X)$ . In each of these situations, the hole is predicted to be broader and more flattened at the bottom than bell-shaped. In [52], the authors removed the surface air pressure from equation (1), and considered the following simplified form to FKdV equation

$$\frac{1}{c} \partial_T \Phi + \left[ (\mathcal{F}_r - 1) - \frac{3}{2} \frac{\Phi}{h} \right] \partial_X \Phi - \frac{1}{6} h^2 \partial_X^3 \Phi - \frac{1}{2} \partial_X b(X) = 0. \quad (2)$$

By substituting an arbitrary order derivative for the time derivative in the current study, we get the following fractional-order forced KdV (FF-KdV) equation [53]:

$$D_T^\gamma \Phi + c \left[ \left( (\mathcal{F}_r - 1) - \frac{3}{2} \frac{\Phi}{h} \right) \partial_X \Phi - \frac{1}{6} h^2 \partial_X^3 \Phi - \frac{1}{2} \partial_X b(X) \right] = 0, \quad (3)$$

where  $0 < \gamma \leq 1$  and the operator  $D_T^\gamma \equiv \frac{\partial^\gamma}{\partial T^\gamma}$  indicates the Caputo fractional derivative having order  $\gamma$ . In this study, both Yang transform decomposition method (YTDM) and Yang homotopy perturbation method (YHPM) are introduced for analyzing the FF-KdV (3). The proposed methods involve the combination of the Yang transform (YT) with the homotopy perturbation technique (HPM) to produce the (YTHPM), as well as the combination of the adomian decomposition method (ADM) with YT to generate the (YTADM). These methods are used to obtain analytical approximations for non-integer evolution equations. It is known that the HPM was introduced for the first time by He [54, 55] in 1998, which in this technique, the solution is postulated to be the aggregate of an endless series that exhibits quick convergence toward exact outcomes. The mentioned technique has demonstrated efficacy in resolving and examining linear and nonlinear equations. Moreover, to create YTDM, the ADM and the Yang transform are merged. By eliminating the requirement to calculate the fractional integrals

or fractional derivative in the recursive mechanism, the suggested method enables estimating the series terms easier than the conventional Adomian method [56].

The forthcoming parts of the manuscript are organized in the following manner: section 2 comprises a declarative declaration and several fundamental concepts. Sections 3 and 4 delineate the recommended procedures for the proposed techniques. Section 5 contains the application and illustrations for the suggested approach. Section 6 outlines the investigation's conclusion.

**2. Preliminaries**

Below are the definitions of Caputo's fractional derivative and various features of YT:

*2.1. Definition*

In the context of the Caputo sense, the fractional-order derivative is defined as follows

$$D_T^\gamma \Phi = \frac{1}{\Gamma(k - \gamma)} \int_0^T (T - \vartheta)^{k-\gamma-1} \Phi^{(k)} d\vartheta,$$

where  $k - 1 < \gamma \leq k, k \in \mathbb{N}$ , and  $\Phi \equiv \Phi(X, T)$ .

*2.2. Definition*

The YT of a function  $\Phi(T)$  is defined as

$$\mathbf{Y}\{\Phi(T)\} = M(u) = \int_0^\infty e^{-\frac{T}{u}} \Phi(T) dT, \quad T > 0, \quad u \in (-T_1, T_2), \tag{4}$$

with the inverse YT

$$\mathbf{Y}^{-1}\{M(u)\} = \Phi(T). \tag{5}$$

*2.3. Definition*

The YT of the function  $\Phi^n(T)$  with  $n$ th derivative reads

$$\mathbf{Y}\{\Phi^n(T)\} = \frac{M(u)}{u^n} - \sum_{k=0}^{n-1} \frac{\Phi^{(k)}(0)}{u^{n-k-1}}, \quad \forall n = 1, 2, 3, \dots \tag{6}$$

*2.4. Definition*

The YT of the fractional-order derivative function  $\Phi^\gamma(T)$  is given by

$$\mathbf{Y}\{\Phi^\gamma(T)\} = \frac{M(u)}{u^\gamma} - \sum_{k=0}^{n-1} \frac{\Phi^{(k)}(0)}{u^{\gamma-(k+1)}}, \quad 0 < \gamma \leq n. \tag{7}$$

**3. Analysis of HPTM**

We can provide the fundamental aspects of HPTM in the following points to comprehend the process of its application to the problem under study. To start, let us introduce the

following problem

$$\begin{cases} D_T^\gamma \Phi = \mathcal{P}_1[X]\Phi + \mathcal{Q}_1[X]\Phi, \\ \Phi(X, 0) = \xi(X), \end{cases} \tag{8}$$

where  $0 < \gamma \leq 1, \Phi \equiv \Phi(X, T), D_T^\gamma = \frac{\partial^\gamma}{\partial T^\gamma}$  indicates the Caputo fractional derivative,  $\mathcal{P}_1[X]$  and  $\mathcal{Q}_1[X]$ , respectively, are the linear and nonlinear operators. On taking YT of either sides

$$\mathbf{Y}[D_T^\gamma \Phi] = \mathbf{Y}[\mathcal{P}_1[X]\Phi + \mathcal{Q}_1[X]\Phi], \tag{9}$$

$$\frac{1}{u^\gamma} \{M(u) - u\Phi(0)\} = \mathbf{Y}[\mathcal{P}_1[X]\Phi + \mathcal{Q}_1[X]\Phi], \tag{10}$$

which leads to

$$M(u) = u\Phi(0) + u^\gamma \mathbf{Y}[\mathcal{P}_1[X]\Phi + \mathcal{Q}_1[X]\Phi]. \tag{11}$$

Implementing the inverse YT on either sides

$$\Phi = \Phi(0) + \mathbf{Y}^{-1}[u^\gamma \mathbf{Y}[\mathcal{P}_1[X]\Phi + \mathcal{Q}_1[X]\Phi]]. \tag{12}$$

Now, we proceed to apply the perturbation technique

$$\Phi = \sum_{k=0}^\infty \epsilon^k \Phi_k, \tag{13}$$

with parameter  $\epsilon \in [0, 1]$  and  $\Phi_k \equiv \Phi_k(X, T)$ .

The breakdown of nonlinear term is given by

$$\mathcal{Q}_1[X]\Phi = \sum_{k=0}^\infty \epsilon^k H_n(\Phi), \tag{14}$$

with  $H_k(\Phi)$  illustrating He's polynomials and given by

$$H_n(\Phi_0, \Phi_1, \dots, \Phi_n) = \frac{1}{\Gamma(n+1)} D_\epsilon^n \left[ \mathcal{Q}_1 \left( \sum_{k=0}^\infty \epsilon^k \Phi_k \right) \right]_{\epsilon=0}, \tag{15}$$

where  $D_\epsilon^k = \frac{\partial^k}{\partial \epsilon^k}$ . Using equations (11) and (12) in equation (10), we have

$$\sum_{k=0}^\infty \epsilon^k \Phi_k(X, T) = \Phi(0) + \epsilon \left( \mathbf{Y}^{-1} \left[ u^\gamma \mathbf{Y} \left\{ \mathcal{P}_1 \sum_{k=0}^\infty \epsilon^k \Phi_k(X, T) + \sum_{k=0}^\infty \epsilon^k H_k(\Phi) \right\} \right] \right). \tag{16}$$

By matching either sides of the above equation in terms of power of  $\epsilon$ , we get

$$\begin{aligned} \epsilon^0: & \Phi_0(X, T) = \Phi(0), \\ \epsilon^1: & \Phi_1(X, T) = \mathbf{Y}^{-1}[u^\gamma \mathbf{Y}[\mathcal{P}_1[X]\Phi_0(X, T) + H_0(\Phi)]], \\ \epsilon^2: & \Phi_2(X, T) = \mathbf{Y}^{-1}[u^\gamma \mathbf{Y}[\mathcal{P}_1[X]\Phi_1(X, T) + H_1(\Phi)]], \\ & \vdots \\ \epsilon^k: & \Phi_k(X, T) = \mathbf{Y}^{-1}[u^\gamma \mathbf{Y}[\mathcal{P}_1[X]\Phi_{k-1}(X, T) + H_{k-1}(\Phi)]], \end{aligned} \tag{17}$$

where  $k > 0$  and  $k \in \mathbb{N}$ .

Lastly, the approximate solution  $\Phi_k(X, T)$  reads

$$\Phi(X, T) = \lim_{M \rightarrow \infty} \sum_{k=1}^M \Phi_k(X, T). \tag{18}$$

#### 4. Analysis of YTDM

The following problem is considered to demonstrate the core theory and solution process of YTDM

$$\begin{cases} D_T^\gamma \Phi = \mathcal{P}_1 + \mathcal{Q}_1, \\ \Phi(X, 0) = \Phi(X), \end{cases} \tag{19}$$

where  $0 < \gamma \leq 1$  and  $D_T^\gamma = \frac{\partial^\gamma}{\partial T^\gamma}$  signifies the Caputo fractional derivative,  $\mathcal{P}_1 \equiv \mathcal{P}_1(X, T)$  and  $\mathcal{Q}_1 \equiv \mathcal{Q}_1(X, T)$ , respectively, are the linear and nonlinear operators, and  $\Phi \equiv \Phi(X, T)$ . By taking YT for either sides, we get

$$\mathbf{Y}[D_T^\gamma \Phi] = \mathbf{Y}[\mathcal{P}_1 + \mathcal{Q}_1], \tag{20}$$

$$\frac{1}{u^\gamma} \{M(u) - u\Phi(0)\} = \mathbf{Y}[\mathcal{P}_1 + \mathcal{Q}_1], \tag{21}$$

which leads to

$$M(\Phi) = u\Phi(0) + u^\gamma \mathbf{Y}[\mathcal{P}_1 + \mathcal{Q}_1]. \tag{22}$$

Implementing the inverse YT on either sides, we have

$$\Phi = \Phi(0) + \mathbf{Y}^{-1}[u^\gamma \mathbf{Y}[\mathcal{P}_1 + \mathcal{Q}_1]]. \tag{23}$$

The solution by means of infinite sequence is as

$$\Phi(X, T) = \sum_{m=0}^{\infty} \Phi_m(X, T). \tag{24}$$

The nonlinear terms are illustrated through Adomian polynomials as

$$\mathcal{Q}_1(X, T) = \sum_{m=0}^{\infty} \mathcal{A}_m. \tag{25}$$

The breakdown of nonlinear term reads

$$\mathcal{A}_m = \frac{1}{m!} \left[ \frac{\partial^m}{\partial \ell^m} \left\{ \mathcal{Q}_1 \left( \sum_{k=0}^{\infty} \ell^k X_k, \sum_{k=0}^{\infty} \ell^k T_k \right) \right\} \right]_{\ell=0}. \tag{26}$$

Using equations (23) and (25) into (22), we get

$$\begin{aligned} \sum_{m=0}^{\infty} \Phi_m(X, T) &= \Phi(0) + \mathbf{Y}^{-1} u^\gamma \left[ \mathbf{Y} \left\{ \mathcal{P}_1 \left( \sum_{m=0}^{\infty} X_m, \sum_{m=0}^{\infty} T_m \right) \right. \right. \\ &\left. \left. + \sum_{m=0}^{\infty} \mathcal{A}_m \right\} \right]. \end{aligned} \tag{27}$$

By matching either sides of the above equation, we obtain

$$\Phi_0(X, T) = \Phi(0), \tag{28}$$

$$\Phi_1(X, T) = \mathbf{Y}^{-1}[u^\gamma \mathbf{Y}\{\mathcal{P}_1(X_0, T_0) + \mathcal{A}_0\}]. \tag{29}$$

Finally, the general terms for  $m \geq 1$  reads

$$\Phi_{m+1}(X, T) = \mathbf{Y}^{-1}[u^\gamma \mathbf{Y}\{\mathcal{P}_1(X_m, T_m) + \mathcal{A}_m\}]. \tag{30}$$

#### 5. Applications

In this segment, we deal with the HPTM and YTDM to find some analytical solutions to the FF-KdV equation.

Let us suppose, the following FF-KdV equation [52, 53]

$$\begin{aligned} D_T^\gamma \Phi + c \left[ \left( (\mathcal{F}_r - 1) - \frac{3\Phi}{2h} \right) \partial_X \Phi - \frac{1}{6} h^2 \partial_X^3 \Phi \right. \\ \left. + \frac{1}{2} \partial_X (1 + 0.1e^{-\frac{X^n}{4}}) \right] = 0, \end{aligned} \tag{31}$$

with initial solution

$$\Phi(X, 0) = -\frac{2e^X}{(1 + e^X)^2},$$

where  $\Phi \equiv \Phi(X, T)$  and  $\gamma \in (0, 1]$ .

##### 5.1. Anatomy the FF-KdV equation using HPTM

By taking YT for equation (31), we have

$$\begin{aligned} \mathbf{Y}\{D_T^\gamma \Phi\} = -c \mathbf{Y} \left\{ \left[ \left( (\mathcal{F}_r - 1) - \frac{3\Phi}{2h} \right) \partial_X \Phi \right. \right. \\ \left. \left. - \frac{1}{6} h^2 \partial_X^3 \Phi + \frac{1}{2} \partial_X (1 + 0.1e^{-\frac{X^n}{4}}) \right] \right\}, \end{aligned} \tag{32}$$

$$\begin{aligned} \frac{1}{u^\gamma} \{M(u) - u\Phi(0)\} = -c \mathbf{Y} \left\{ \left[ \left( (\mathcal{F}_r - 1) - \frac{3\Phi}{2h} \right) \partial_X \Phi \right. \right. \\ \left. \left. - \frac{1}{6} h^2 \partial_X^3 \Phi + \frac{1}{2} \partial_X (1 + 0.1e^{-\frac{X^n}{4}}) \right] \right\}, \end{aligned} \tag{33}$$

which leads to

$$\begin{aligned} M(u) = u\Phi(0) - cu^\gamma \mathbf{Y} \left\{ \left[ \left( (\mathcal{F}_r - 1) - \frac{3\Phi}{2h} \right) \partial_X \Phi \right. \right. \\ \left. \left. - \frac{1}{6} h^2 \partial_X^3 \Phi + \frac{1}{2} \partial_X (1 + 0.1e^{-\frac{X^n}{4}}) \right] \right\}. \end{aligned} \tag{34}$$

Implementing the inverse YT to equation (34), we get

$$\begin{aligned} \Phi = \Phi(0) - c \mathbf{Y}^{-1} \left[ u^\gamma \left\{ \mathbf{Y} \left( \left( (\mathcal{F}_r - 1) - \frac{3\Phi}{2h} \right) \partial_X \Phi \right. \right. \right. \\ \left. \left. - \frac{1}{6} h^2 \partial_X^3 \Phi + \frac{1}{2} \partial_X (1 + 0.1e^{-\frac{X^n}{4}}) \right) \right\} \right], \end{aligned} \tag{35}$$

which equivalent

$$\begin{aligned} \Phi = -\frac{2e^X}{(1 + e^X)^2} - c \mathbf{Y}^{-1} \left[ u^\gamma \left\{ \mathbf{Y} \left( \left( (\mathcal{F}_r - 1) - \frac{3\Phi}{2h} \right) \partial_X \Phi \right. \right. \right. \\ \left. \left. - \frac{1}{6} h^2 \partial_X^3 \Phi + \frac{1}{2} \partial_X (1 + 0.1e^{-\frac{X^n}{4}}) \right) \right\} \right]. \end{aligned} \tag{36}$$

Now, by applying the perturbation technique, we have

$$\begin{aligned} \sum_{k=0}^{\infty} \epsilon^k \Phi_k = -\frac{2e^X}{(1 + e^X)^2} - c \mathbf{Y}^{-1} \\ \times \left[ u^\gamma \left\{ \mathbf{Y} \left( \left( (\mathcal{F}_r - 1) \sum_{k=0}^{\infty} \epsilon^k \Phi_k \right) \frac{3}{2h} \sum_{k=0}^{\infty} \epsilon^k H_k(\Phi) \right. \right. \right. \\ \left. \left. - \frac{1}{6} h^2 \partial_X^3 \left( \sum_{k=0}^{\infty} \epsilon^k \Phi_k \right) + \frac{1}{2} \partial_X (0.1e^{-\frac{X^n}{4}} + 1) \right) \right\} \right], \end{aligned} \tag{37}$$

where  $\Phi_k \equiv \Phi_k(X, T)$ .

Some nonlinear terms are calculated as follows

$$\begin{aligned} H_0(\Phi) &= \Phi_0(\Phi_0)_X, \\ H_1(\Phi) &= \Phi_1(\Phi_0)_X + \Phi_0(\Phi_1)_X, \\ &\vdots \end{aligned} \tag{38}$$

By matching either sides of the above equation in terms of power of  $\epsilon$ , we have

$$\begin{aligned} \epsilon^0: \Phi_0(X, T) &= -\frac{2e^X}{(1+e^X)^2}, \\ \epsilon^1: \Phi_1(X, T) &= -\frac{T^\gamma c}{\Gamma(\gamma+1)} \left[ \frac{6e^{2X}(-1+e^X)}{(1+e^X)^5 h} \right. \\ &\quad \left. - \frac{e^X(-1+11e^X-11e^{2X}+e^{3X})h^2}{3(1+e^X)^5} \right. \\ &\quad \left. - 0.0125nX^{-1+n}e^{-\frac{X^n}{4}} + \frac{2e^X(-1+e^X)(-1+\mathcal{F}_r)}{(-1+e^X)^3} \right]. \\ &\quad \vdots \end{aligned} \tag{39}$$

Finally, the approximate solution until second-order approximation reads

Finally, the approximate solution until the second-order approximation can be obtained by inserting the values of  $\Phi_0(X, T)$  and  $\Phi_1(X, T)$  given in system (39) into the following form solution

$$\Phi(X, T) = \sum_{m=0}^{\infty} \Phi_m(X, T) = \Phi_0(X, T) + \Phi_1(X, T) + \dots \tag{40}$$

### 6. Anatomy of the FF-KdV equation using YTDM

Now, by taking the YT of both sides of problem (31), we get:

$$\begin{aligned} \mathbf{Y}\{D_T^\gamma \Phi\} &= -c\mathbf{Y}\left\{\left[\left(\mathcal{F}_r - 1\right) - \frac{3\Phi}{2h}\right]\partial_X\Phi \right. \\ &\quad \left. - \frac{1}{6}h^2\partial_X^3\Phi + \frac{1}{2}\partial_X(1 + 0.1e^{-\frac{X^n}{4}})\right\}, \end{aligned} \tag{41}$$

which leads to

$$\begin{aligned} \frac{1}{u^\gamma}\{M(u) - u\Phi(0)\} &= -c\mathbf{Y}\left\{\left[\left(\mathcal{F}_r - 1\right) - \frac{3\Phi}{2h}\right]\partial_X\Phi \right. \\ &\quad \left. - \frac{1}{6}h^2\partial_X^3\Phi + \frac{1}{2}\partial_X(1 + 0.1e^{-\frac{X^n}{4}})\right\}, \end{aligned} \tag{42}$$

and finally, we get

$$\begin{aligned} M(u) &= u\Phi(0) - cu\mathbf{Y}\left\{\left[\left(\mathcal{F}_r - 1\right) - \frac{3\Phi}{2h}\right]\partial_X\Phi \right. \\ &\quad \left. - \frac{1}{6}h^2\partial_X^3\Phi + \frac{1}{2}\partial_X(1 + 0.1e^{-\frac{X^n}{4}})\right\}. \end{aligned} \tag{43}$$

Implementing the inverse YT for both sides of problem (43),

we have

$$\begin{aligned} \Phi &= \Phi(0) - c\mathbf{Y}^{-1}\left[u^\gamma\left\{\mathbf{Y}\left[\left(\mathcal{F}_r - 1\right) - \frac{3\Phi}{2h}\right]\partial_X\Phi \right. \right. \\ &\quad \left. \left. - \frac{1}{6}h^2\partial_X^3\Phi \right. \right. \\ &\quad \left. \left. + \frac{1}{2}\partial_X(1 + 0.1e^{-\frac{X^n}{4}})\right\}\right], \end{aligned} \tag{44}$$

which equivalents  $\mu$

$$\begin{aligned} \Phi &= -\frac{2e^X}{(1+e^X)^2} - c\mathbf{Y}^{-1}\left[u^\gamma\left\{\mathbf{Y}\left[\left(\mathcal{F}_r - 1\right) - \frac{3\Phi}{2h}\right]\partial_X\Phi \right. \right. \\ &\quad \left. \left. - \frac{1}{6}h^2\partial_X^3\Phi + \frac{1}{2}\partial_X(1 + 0.1e^{-\frac{X^n}{4}})\right\}\right]. \end{aligned} \tag{45}$$

The solution by means of infinite sequence reads

$$\Phi(X, T) = \sum_{m=0}^{\infty} \Phi_m(X, T). \tag{46}$$

By using equation (46) and the Adomian polynomials for nonlinear term as given in equation (25). Hence, solution (44), simplifies to

$$\begin{aligned} \sum_{m=0}^{\infty} \Phi_m(X, T) &= \Phi(0) - c\mathbf{Y}^{-1} \\ &\quad \times \left[ u^\gamma \left\{ \mathbf{Y} \left[ \left( \mathcal{F}_r - 1 \right) \partial_X \Phi \right] \frac{3}{2h} \sum_{m=0}^{\infty} \mathcal{A}_m - \frac{1}{6} h^2 \partial_X^3 \Phi \right. \right. \\ &\quad \left. \left. + \frac{1}{2} \partial_X (1 + 0.1 e^{-\frac{X^n}{4}}) \right\} \right], \end{aligned} \tag{47}$$

which equivalents

$$\begin{aligned} \sum_{m=0}^{\infty} \Phi_m(X, T) &= -\frac{2e^X}{(1+e^X)^2} - c\mathbf{Y}^{-1} \\ &\quad \times \left[ u^\gamma \left\{ \mathbf{Y} \left[ \left( \mathcal{F}_r - 1 \right) \partial_X \Phi \right] \frac{3}{2h} \sum_{m=0}^{\infty} \mathcal{A}_m \right. \right. \\ &\quad \left. \left. - \frac{1}{6} h^2 \partial_X^3 \Phi + \frac{1}{2} \partial_X (1 + 0.1 e^{-\frac{X^n}{4}}) \right\} \right]. \end{aligned} \tag{48}$$

Some nonlinear terms are presented as follows:

$$\begin{aligned} H_0(\Phi) &= \Phi_0(\Phi_0)_X, \\ H_1(\Phi) &= \Phi_1(\Phi_0)_X + \Phi_0(\Phi_1)_X, \\ &\quad \vdots \end{aligned} \tag{49}$$

By matching either sides of the above equation, we get

$$\Phi_0(X, T) = -\frac{2e^X}{(1+e^X)^2}, \tag{50}$$

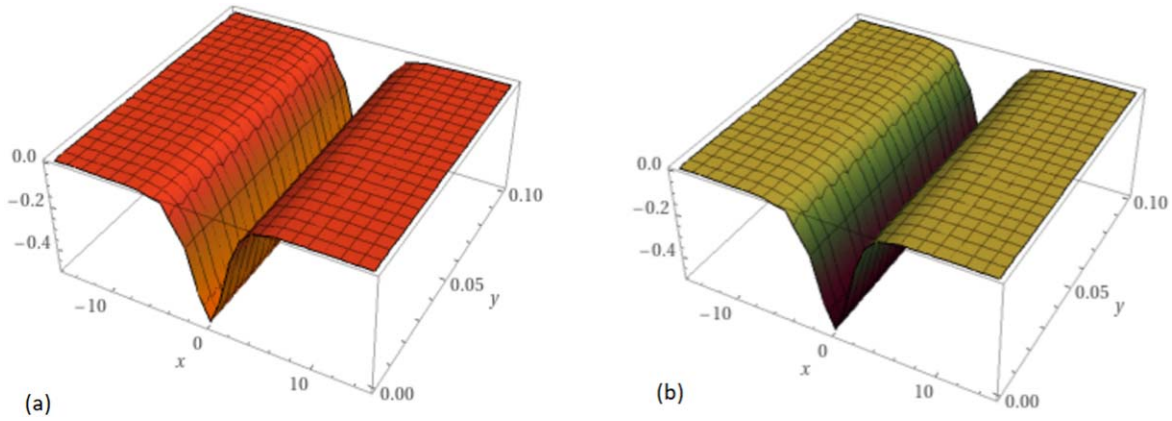


**Figure 1.** The two approximations (40) and (52) are examined for the integer case  $\gamma = 1$  at  $(\mathcal{F}_r, n) = (-1, 2)$ : (a) the approximation (40) using HPTM (b) the approximation (52) using YTDM.

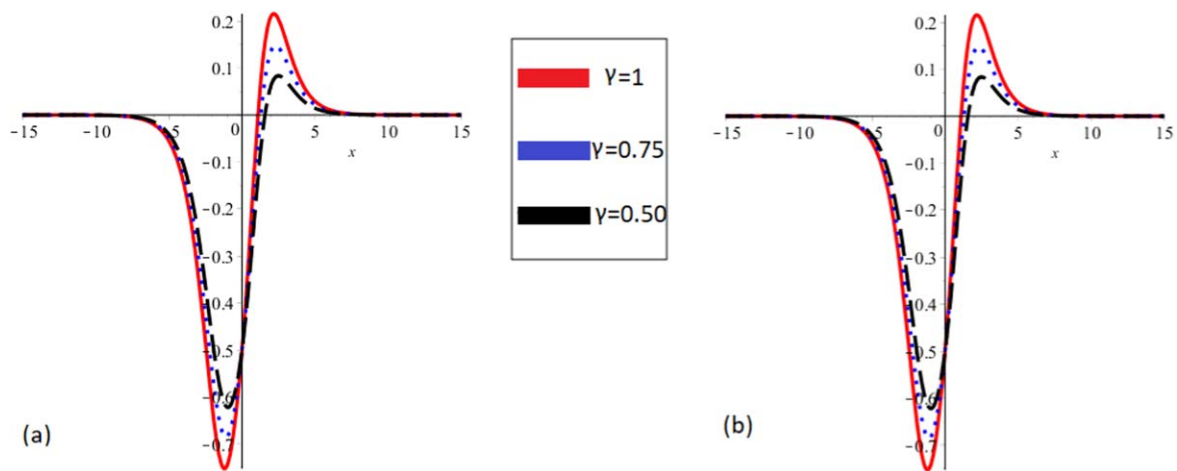


**Figure 2.** The behavior of the two approximations (40) and (52) are plotted against the fractional parameter  $\gamma$  at  $(\mathcal{F}_r, n) = (-1, 2)$ : (a) the approximation (40) using HPTM (b) the approximation (52) using YTDM.

for  $m = 0$ , and for  $m = 1$ , we have

$$\begin{aligned} \Phi_1(X, T) = & -\frac{T^\gamma c}{\Gamma(\gamma + 1)} \left[ \frac{6e^{2X}(-1 + e^X)}{(1 + e^X)^5 h} \right. \\ & - \frac{e^X(-1 + 11e^X - 11e^{2X} + e^{3X})h^2}{3(1 + e^X)^5} \\ & \left. - 0.0125nX^{-1+n}e^{-\frac{X^n}{4}} + \frac{2e^X(-1 + e^X)(-1 + \mathcal{F}_r)}{(-1 + e^X)^3} \right]. \end{aligned} \quad (51)$$

Finally, the YTDM approximation for  $(m \geq 1)$  can be calculated in the same manner. Thus, the approximate solution until the second-order approximation can be obtained by inserting the values of  $\Phi_0(X, T)$  and  $\Phi_1(X, T)$  given, respectively, in equations (50) and (51) into the following form solution

$$\Phi(X, T) = \sum_{m=0}^{\infty} \Phi_m(X, T) = \Phi_0(X, T) + \Phi_1(X, T) + \dots \quad (52)$$

We perform a quantitative examination for solutions (40) and (52) derived using the HPTM and YTDM, respectively, to clearly illustrate and understand the effect of different physical and fractional parameters on their behavior. For the integer case ( $\gamma = 1$ ), the two approximations (40) and

(52) are graphically analyzed as illustrated in figures 1(a) and (b), respectively. Moreover, at  $(\mathcal{F}_r, n) = (-1, 2)$ , the two approximations (40) and (52) are compared with each other at different values for the fractional parameter  $\gamma$  as illustrated in figures 2(a) and (b), respectively. This comparative study highlights the sensitivity of the models to different values of fractional parameter  $\gamma$ , providing insights into the optimal conditions for each model's performance. Moreover, the two approximation (40) and (52) at  $(\mathcal{F}_r, n) = (-1, 4)$  and for the integer case ( $\gamma = 1$ ) are numerically investigated as illustrated in figures 3(a) and (b), respectively. Also, at  $(\mathcal{F}_r, n) = (-1, 4)$ , the impact of the fractional parameter  $\gamma$  on the two approximations (40) and (52) are numerically examined as evident in figures 4(a) and (b), respectively. Furthermore, the numerical investigation of the two approximations (40) and (52) for the integer case ( $\gamma = 1$ ) and for  $(\mathcal{F}_r, n) = (-1, 8)$  is depicted in figures 5(a) and (b), respectively. Additionally, the numerical analysis of the effect of the fractional parameter  $\gamma$  on the two approximations (40) and (52) is conducted at  $(\mathcal{F}_r, n) = (-1, 8)$ , as seen in figures 6(a) and (b), respectively. The results highlight the effect of the fractional parameter on the profile of the SWs, which contributes significantly to understanding the behavior

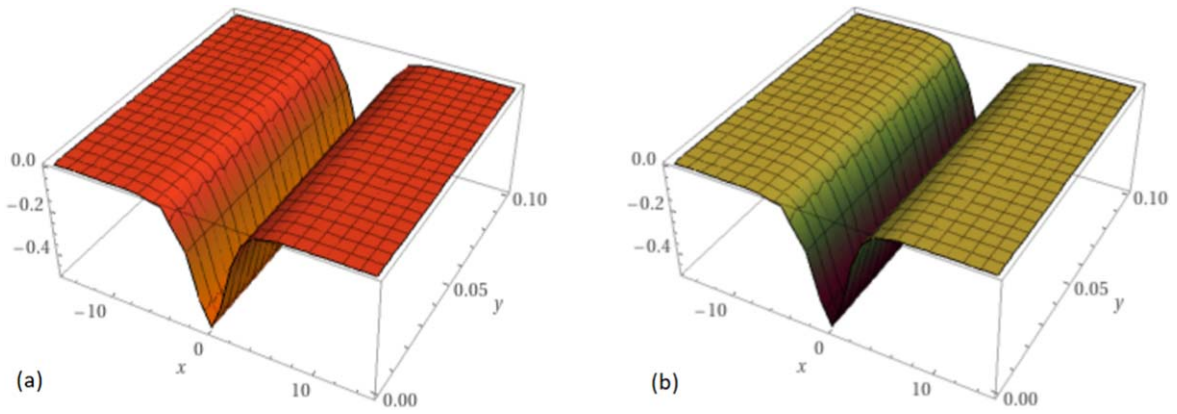


**Figure 3.** The two approximations (40) and (52) are examined for the integer case  $\gamma = 1$  at  $(\mathcal{F}_r, n) = (-1, 4)$ : (a) the approximation (40) using HPTM (b) The approximation (52) using YTDM.

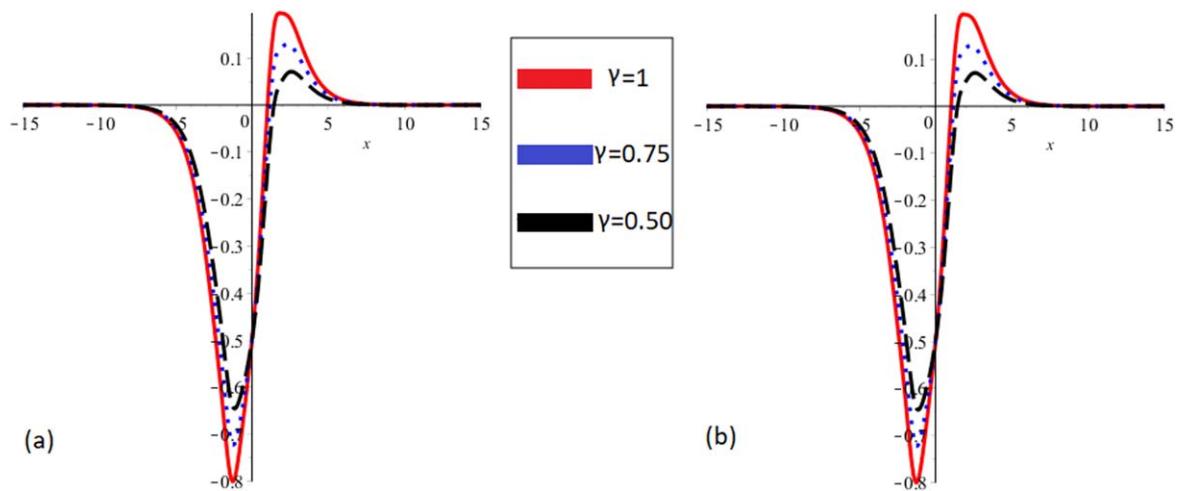


**Figure 4.** The behavior of the two approximations (40) and (52) are plotted against the fractional parameter  $\gamma$  at  $(\mathcal{F}_r, n) = (-1, 4)$ : (a) the approximation (40) using HPTM (b) the approximation (52) using YTDM.

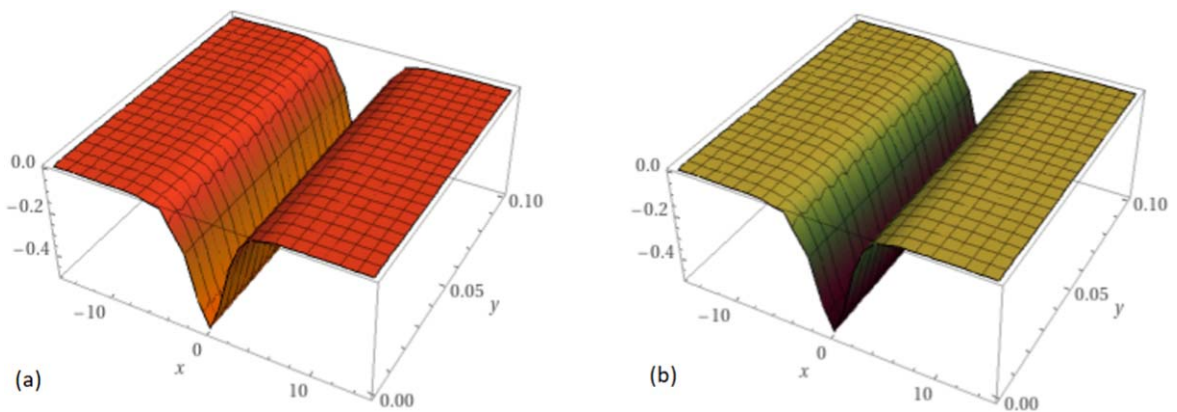


**Figure 5.** The two approximations (40) and (52) are examined for the integer case  $\gamma = 1$  at  $(\mathcal{F}_r, n) = (-1, 8)$ : (a) the approximation (40) using HPTM (b) the approximation (52) using YTDM.

of these waves. For  $(\gamma, n) = (1, 8)$ , the impact of Froude number  $F_r$  on the SW profile according to both HPTM and YTDM are examined as illustrated in figures 7(a) and (b), respectively.

Ultimately, the derived approximations using both HPTM and YTDM approaches are characterized by high

accuracy and stability at large study domain values. These methods are also characterized by simplicity and avoid many mathematical complications that may result from other methods. The obtained approximations also accurately describe the solitary waves and how the fractional parameter impacts their profile.

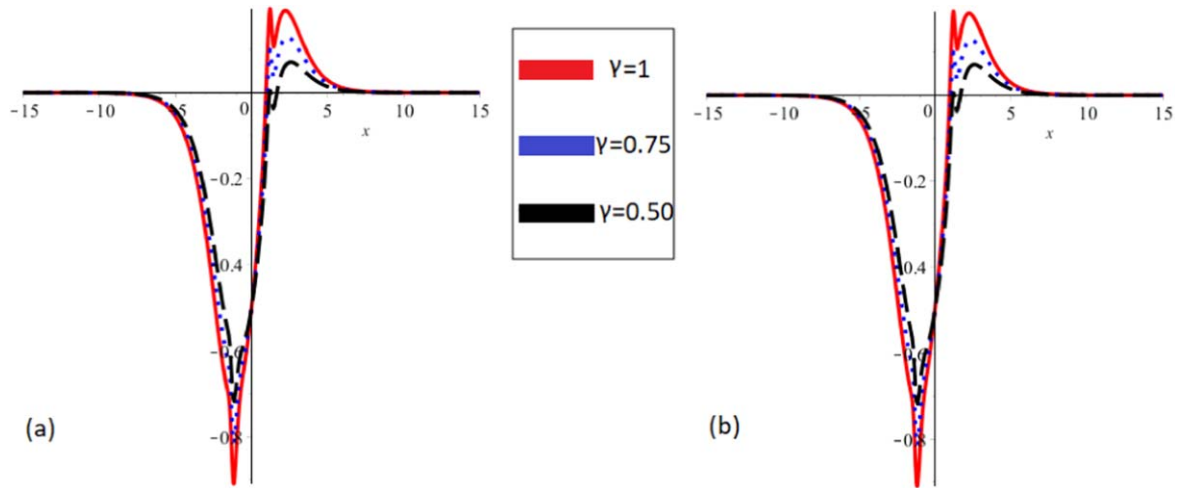


**Figure 6.** The behavior of the two approximations (40) and (52) are plotted against the fractional parameter  $\gamma$  at  $(\mathcal{F}_r, n) = (-1, 8)$ : (a) the approximation (40) using HPTM (b) the approximation (52) using YTDM.

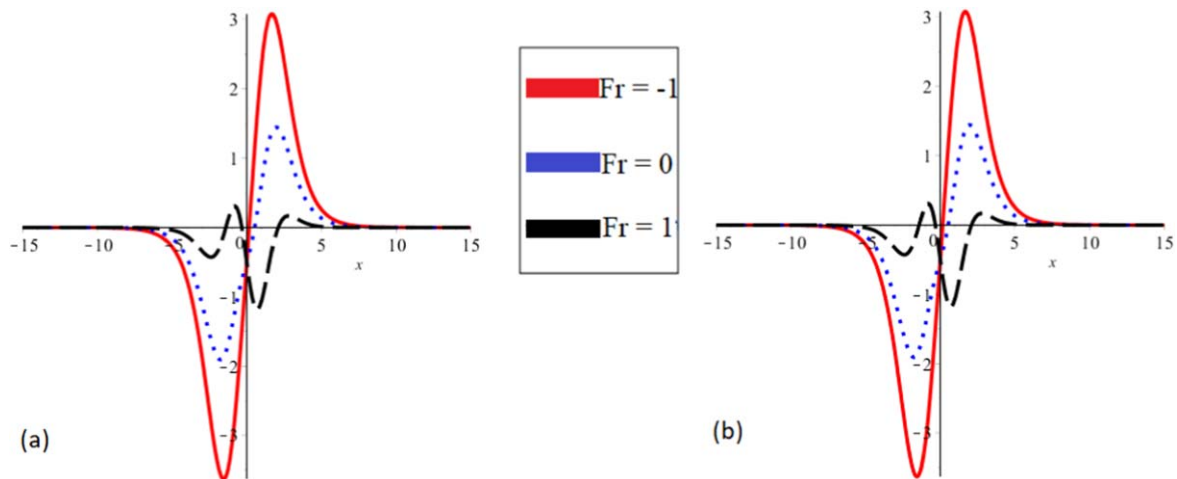


**Figure 7.** The behavior of the two approximations (40) and (52) are plotted against the Froude number  $\mathcal{F}_r$  at  $(\gamma, n) = (1, 8)$ : (a) the approximation (40) using HPTM (b) the approximation (52) using YTDM.

**7. Conclusion**

In this investigation, the fractional forced Korteweg–de Vries (FF-KdV) equation has been analyzed using YTDM and YHPM in the framework of Caputo operator. Two analytical approximations have been derived using the proposed techniques. The generated approximations have undergone numerical analysis using specific numerical values for the relevant parameters. The numerical analysis results exhibited a notable level of precision in the derived approximations. This was evident when comparing these approximations with the precise analytical solutions of the integer case and between these approximations themselves. Based on the recommended methodologies for addressing the stated issue, it has been verified that the mathematical model of fractional order exhibits superior accuracy in interpreting experimental data compared to the integer-order model.

The obtained results showcase the robustness of suggested techniques in terms of accuracy and their extensive range of applicability to problems involving fractional

nonlinear dynamics. Therefore, these techniques can be utilized to examine diverse forms of nonlinear problems that inherently arise in real-world scenarios, especially to analyze many nonlinear evolution equations used to describe various nonlinear structures in different plasma models.

Future work: it is necessary to examine and analyze various fractional nonlinear evolution equations related to various plasma models to reveal the ambiguity around some phenomena that arise in different plasma models. For instance, the damped FF-KdV equation, nonplanar FF-KdV equation, damped nonplanar FF-KdV equation, and many other related equations with higher-order nonlinearity and dispersion should be investigated [37–44].

**Acknowledgments**

The authors express their gratitude to Princess Nourah bint Abdulrahman University Researchers Supporting Project

number (PNURSP2024R229), Princess Nourah bint Abdulrahman University, Riyadh, Saudi Arabia.

### Conflict of interest

The authors declare that they have no conflicts of interest.

### Authors contributions

All authors contributed equally and approved the final version of the current manuscript.

### References

- [1] Ionescu C, Lopes A, Copot D, Machado J T and Bates J H 2017 The role of fractional calculus in modeling biological phenomena: a review *Commun. Nonlinear Sci. Numer. Simul.* **51** 141–59
- [2] Sinan M, Shah K, Kumam P, Mahariq I, Ansari K J, Ahmad Z and Shah Z 2022 Fractional order mathematical modeling of typhoid fever disease *Results Phys.* **32** 105044
- [3] Wu S L and Al-Khaleel M 2016 Convergence analysis of the Neumann–Neumann waveform relaxation method for time-fractional RC circuits *Simul. Modell. Pract. Theor.* **64** 43–56
- [4] Arora S, Mathur T, Agarwal S, Tiwari K and Gupta P 2022 Applications of fractional calculus in computer vision: a survey *Neurocomputing* **489** 407–28
- [5] Area I and Nieto J J 2021 Power series solution of the fractional logistic equation *PhysicaA* **573** 125947
- [6] Wu S L and Al-Khaleel M 2017 Parameter optimization in waveform relaxation for fractional-order RC circuits *IEEE Trans. Circuits Syst.I* **64** 1781–90
- [7] Baleanu D, Guevenc Z B and Machado J A T 2010 *New Trends in Nanotechnology and Fractional Calculus Applications* (Springer) (<https://doi.org/10.1007/978-90-481-3293-5>)
- [8] Sweilam N H, Hasan M M A and Baleanu D 2017 New studies for general fractional financial models of awareness and trial advertising decisions *Chaos Solitons Fractals* **104** 772–84
- [9] Baleanu D, Wu G C and Zeng S D 2017 Chaos analysis and asymptotic stability of generalized Caputo fractional differential equations *Chaos Solitons Fractals* **102** 99–105
- [10] Veerasha P, Prakasha D G and Baskonus H M 2019 New numerical surfaces to the mathematical model of cancer chemotherapy effect in Caputo fractional derivatives *Chaos* **29** 013119
- [11] Noor S, Alyousef H A, Shafee A, Shah R and El-Tantawy S A 2024 A novel analytical technique for analyzing the (3+1)-dimensional fractional calogero- bogoyavlenskii-schiff equation: investigating solitary/shock waves and many others physical phenomena *Phys. Scr.* **99** 065257
- [12] Goufo E F D 2016 Application of the Caputo–Fabrizio fractional derivative without singular kernel to Korteweg–de Vries–Burgers equation *Math. Model. Numer. Anal.* **21** 188–98
- [13] Kilbas A A, Srivastava H M and Trujillo J J 2006 *Theory and Applications of Fractional Differential Equations* vol 204 (Elsevier) ([https://doi.org/10.1016/S0304-0208\(06\)80001-0](https://doi.org/10.1016/S0304-0208(06)80001-0))
- [14] Sun H, Zhang Y, Baleanu D, Chen W and Chen Y 2018 A new collection of real world applications of fractional calculus in science and engineering *Commun. Nonlinear Sci. Numer. Simul.* **64** 213–31
- [15] Debnath L 2003 Recent applications of fractional calculus to science and engineering *Int. J. Math. Math. Sci.* **2003** 3413–42
- [16] Abu Arqub O 2020 Numerical simulation of time-fractional partial differential equations arising in fluid flows via reproducing Kernel method *Int. J. Numer. Methods Heat Fluid Flow* **30** 4711–33
- [17] Zayed E M, Amer Y A and Shohib R M 2016 The fractional complex transformation for nonlinear fractional partial differential equations in the mathematical physics *J. Assoc. Arab Univ. Basic Appl. Sci.* **19** 59–69
- [18] Shah K, Seadawy A R and Arfan M 2020 Evaluation of one dimensional fuzzy fractional partial differential equations *Alexandria Eng. J.* **59** 3347–53
- [19] Khan H, Shah R, Gómez-Aguilar J F, Baleanu D and Kumam P 2021 Travelling waves solution for fractional-order biological population model *Math. Modell. Nat. Phenom.* **16** 32
- [20] Duffy D J 2013 *Finite Difference Methods in Financial Engineering: A Partial Differential Equation Approach* (Wiley) (<https://doi.org/10.1002/9781118673447>)
- [21] Jeffrey A and Mohamad M N B 1991 Exact solutions to the KdV–Burgers equation *Wave Motion* **14** 369–75
- [22] Goufo E F D and Kumar S 2017 Shallow water wave models with and without singular kernel: existence, uniqueness, and similarities *Math. Probl. Eng.* **2017** 1–9
- [23] Zhang W, Chang Q and Jiang B 2002 Explicit exact solitary-wave solutions for compound KdV-type and compound KdV–Burgers-type equations with nonlinear terms of any order *Chaos Solitons Fractals* **13** 311–9
- [24] Shan Tariq M, Masood W, Siddiq M, Asghar S, Alotaibi B M, Ismaeel S M E and El-Tantawy S A 2023 Bäcklund transformation for analyzing a cylindrical Korteweg–de Vries equation and investigating multiple soliton solutions in a plasma *Phys. Fluids* **35** 103105
- [25] Ishaq M, Chen Z-M and Zhao Q 2023 Analysis of nonlinear water wave interaction solutions and energy exchange between different wave modes *Phys. Fluids* **35** 021907
- [26] Batool N, Masood W, Siddiq M, Alrowaily A W, Ismaeel S M E and El-Tantawy S A 2023 Hirota bilinear method and multi-soliton interaction of electrostatic waves driven by cubic nonlinearity in pair-ion-electron plasmas *Phys. Fluids* **35** 033109
- [27] Almutlak S A, Parveen S, Mahmood S, Qamar A, Alotaibi B M and El-Tantawy S A 2023 On the propagation of cnoidal wave and overtaking collision of slow shear Alfvén solitons in low  $\beta$  magnetized plasmas *Phys. Fluids* **35** 075130
- [28] Albalawi W, El-Tantawy S A and Salas A H 2021 On the rogue wave solution in the framework of a Korteweg–de Vries equation *Results Phys.* **30** 104847
- [29] El-Tantawy S A 2016 Nonlinear dynamics of soliton collisions in electronegative plasmas: the phase shifts of the planar KdV-and mKdV-soliton collisions *Chaos Solitons Fractals* **93** 162
- [30] Wazwaz A-M 2003 Compacton solutions of the Kawahara-type nonlinear dispersive equation *Appl. Math. Comput.* **145** 133
- [31] Alyousef H A, Salas A H, Alharthi M R and El-tantawy S A 2022 New periodic and localized traveling wave solutions to a kawahara-type equation: applications to plasma physics *Complexity* **2022** 9942267
- [32] El-Tantawy S A, Salas A H and Alharthi M R 2021 Novel analytical cnoidal and solitary wave solutions of the extended Kawahara equation *Chaos Solitons Fractals* **147** 110965

- [33] Alkhateeb S A, Hussain S, Wedad Albalawi, El-Tantawy S A and El-Awady E I 2023 Dissipative Kawahara ion-acoustic solitary and cnoidal waves in a degenerate magnetorotating plasma *J. Taibah Univ. Sci.* **17** 2187606
- [34] El-Tantawy S A, Salas A H, Alyousef H A and Alharthi M R 2022 Novel exact and approximate solutions to the family of the forced damped Kawahara equation and modeling strong nonlinear waves in a plasma *Chin. J. Phys.* **77** 2454
- [35] El-Tantawy S A, El-Sherif L S, Bakry A M, Alhejaili W and Wazwaz A-M 2022 On the analytical approximations to the nonplanar damped Kawahara equation: cnoidal and solitary waves and their energy *Phys. Fluids* **34** 113103
- [36] El-Tantawy S A, Salas A H and Alharthi M R 2021 Novel analytical cnoidal and solitary wave solutions of the extended Kawahara equation *Chaos Solitons Fractals* **147** 110965
- [37] Kashkari B S, El-Tantawy S A, Salas A H and El-Sherif L S 2020 Homotopy perturbation method for studying dissipative nonplanar solitons in an electronegative complex plasma *Chaos Solitons Fractals* **130** 109457
- [38] Alkhateeb S A, Hussain S, Albalawi W, El-Tantawy S A and El-Awady E I 2023 Dissipative Kawahara ion-acoustic solitary and cnoidal waves in a degenerate magnetorotating plasma *J. Taibah Univ. Sci.* **17** 2187606
- [39] Alharbey R A, Alrefae W R, Malaikah H, Tag-Eldin E and El-Tantawy S A 2023 Novel approximate analytical solutions to the nonplanar modified Kawahara equation and modeling nonlinear structures in electronegative plasmas *Symmetry* **15** 97
- [40] Alharthi M R, Alharbey R A and El-Tantawy S A 2022 Novel analytical approximations to the nonplanar Kawahara equation and its plasma applications *Eur. Phys. J. Plus* **137** 1172
- [41] Ismaeel S M E, Wazwaz A-M, Tag-Eldin E and El-Tantawy S A 2023 Simulation studies on the dissipative modified Kawahara solitons in a complex plasma *Symmetry* **15** 57
- [42] Alyousef H A, Salas A H, Matoog R T and El-Tantawy S A 2022 On the analytical and numerical approximations to the forced damped Gardner Kawahara equation and modeling the nonlinear structures in a collisional plasma *Phys. Fluids* **34** 103105
- [43] Aljahdaly N H and El-Tantawy S A 2022 Novel analytical solution to the damped Kawahara equation and its application for modeling the dissipative nonlinear structures in a fluid medium *J. Ocean Eng. Sci.* **7** 492
- [44] El-Tantawy S A, Salas A H, Alyousef H A and Alharthi M R 2022 Novel exact and approximate solutions to the family of the forced damped Kawahara equation and modeling strong nonlinear waves in a plasma *Chin. J. Phys.* **77** 2454
- [45] Dias F and Vanden-Broeck J M 2002 Generalized critical free-surface flows *J. Eng. Math.* **42** 291–301
- [46] Shen S S 1995 On the accuracy of the stationary forced Korteweg–de Vries equation as a model equation for flows over a bump *Q. Appl. Math.* **53** 701–19
- [47] Camassa R and Wu T 1991 Stability of forced solitary waves *Phil. Trans. R. Soc. A* **337** 429–66
- [48] Zabuski N J and Kruskal M D 1965 Interaction of solitons in a collisionless plasma and the recurrence of initial states *Phys. Rev. Lett.* **15** 240–3
- [49] Crighton D G 1995 Applications of KdV *Acta Appl. Math.* 39–67
- [50] Hereman W 2012 *Shallow Water Waves and Solitary Waves (Mathematics of Complexity and Dynamical Systems)* ed R Meyers (Springer) ([https://doi.org/10.1007/978-0-387-30440-3\\_480](https://doi.org/10.1007/978-0-387-30440-3_480))
- [51] Wu T Y T 1987 Generation of upstream advancing solitons by moving disturbances *J. Fluid Mech.* **184** 75–99
- [52] David V D, Aziz Z A and Salah F 2016 Analytical approximate solution for the forced Korteweg–de Vries (FKdV) on critical flow over a hole using homotopy analysis method *J. Teknologi (Sci. Eng.)* **78** 107–12
- [53] Veerasha P, Prakasha D G and Singh J 2019 Solution for fractional forced KdV equation using fractional natural decomposition method *AIMS Math.* **5** 798–810
- [54] He J H 1999 Homotopy perturbation technique *Comput. Meth. Appl. Mech. Eng.* **178** 257–62
- [55] He J H 2000 A coupling method of a homotopy technique and a perturbation technique for non-linear problems *Int. J. Non Linear Mech.* **35** 37–43
- [56] Adomian G and Rach R 1983 Inversion of nonlinear stochastic operators *J. Math. Anal. Appl.* **91** 39–46